ISTITUTO NAZIONALE DI FISICA NUCLEARE

Gruppo Collegato di Messina

INFN/AE-03/02
23 Maggio 2003

RESPONSE OF AN UNDERWATER CHERENKOV DETECTOR TO SUPERNOVA NEUTRINOS

Ernesto Amato[1], Lucrezia Auditore[1], Renato C. Barnà[1], Vincenzo D'Amico [1], Domenico De Pasquale[1], Antonio Italiano[2], Antonio Trifirò[1], Marina Trimarchi[1]

[1] *Dipartimento di Fisica, Università di Messina, I-98166 Messina, Italy*
[2] *INFN, Gruppo Collegato di Messina, C.da Papardo, Salita Sperone, I-98166 Messina, Italy*

Abstract

We present a complete Monte Carlo simulation of the response of a realistic model of a deep-underwater Cherenkov detector to Supernova neutrinos, referring to the project proposed by the NEMO Collaboration. The various sources of noise are discussed in detail and a statistical treatment of the data is proposed based upon the integration on a properly chosen time interval. The results show that the neutrino flux emitted by a Supernova exploding in our Galaxy can be detected from such a telescope. The possibility of retrieving information on the SN direction from the asymmetry in the emitted Cherenkov light has been considered, showing that this approach does not allow an accurate localization of the ν source.

PACS.: 29.40.k; 97.60.B; 98.70.S

Submitted Astroparticle Physics

Published by ***SIS–Pubblicazioni***
Laboratori Nazionali di Frascati

1 Supernova types and explosion mechanisms

The term "supernova" was originally coined to describe the sudden appearance in the sky of a new star whose luminosity would overwhelm that of all other stars. Now we know that supernovae (SN) are stars that explode at the end of their evolution, and the theory of supernova explosion makes distinction between two fundamental classes [1,2].

A SN Ia occurs when a carbon-oxygen white dwarf accreting mass from a companion star reaches its Chandrasekar limit and begins to collapse. The gravitational collapse primes nuclear fusion of carbon and oxygen to heavier nuclei, and this violent non-equilibrium process leads to the explosion that leaves no remnant except but an expanding nebula.

The physical mechanism that leads to a supernova spectrally classified as Type II (and probably also as Type Ib and Ic) is totally different: a massive star ($M \geq 8 M_{\odot}$) in its late evolutionary state has an onion structure where, going from the outer envelope to the inner core, we find the nuclear fusion of heavier and heavier nuclei. The degenerate inner core is essentially an iron white dwarf whose mass is accreting due to the fusion in act in the outer shell; when the core mass reaches the Chandrasekar limit begins the collapse phase that cannot ignite nuclear fusion because iron is the most stable nucleus. The collapse ends in a bounce when density reaches supranuclear values and an expanding shock wave forms.

At this point two distinct scenarios seem to be possible: the prompt or the delayed explosion mechanism. In the first case the outer stellar envelope is directly expelled by the shock wave in a time scale of few tens of milliseconds. It seems that the prompt mechanism could work only for small enough progenitor stars (up to $\sim 10 M_{\odot}$) and for a "soft" type of equation of state; otherwise the shock wave energy losses due to photodissociation or neutrino emission cause the stall of the shock itself.

These limits are overtaken in the delayed explosion mechanism by means of the neutrino flux that is able to revive the stalled shock front in a time scale of the order of one second [3,4]. The next section will be devoted to the description of that mechanism, in order to evaluate the expected neutrino flux.

2 Neutrinos from supernovae: the adopted models

We know that in a SN event about 3×10^{53} erg of gravitational energy is released and only 1% of it goes as kinetic energy of the ejecta; 99% is emitted as ν and $\overline{\nu}$ of all flavours [5,6].

Regarding the core-collapse SN (i.e. Type II, Ib and Ic) only about 0.01% of the

total energy is released as light, leading to an optical burst much fainter than SN Type Ia. Core-collapse SN are in fact the brightest impulsive sources of low-energy neutrinos.

Since the computational capabilities of the electronic calculators allowed to perform numerical or semi-analytical simulations, a great effort was spent in order to evaluate the dynamical evolution of core collapse and post bounce explosion. Recently astrophysicists have implemented efficient Boltzmann solvers of the neutrino transport equation, that can be inserted in the hydrodynamic simulation of the whole process [7–9]. These spherically symmetric calculations do not reproduce an explosion, because the considered physical processes do not succeed in reviving the stalled shock.

A spherically symmetric simulation including a mixing-length treatment of neutron finger convection, developed by the Livermore group, leads to a successful explosion [10]: starting with a stellar model developed by Woosley and Weaver for a main-sequence $20M_{\odot}$ star, considered as progenitor of SN 1987A, the Livermore group performed a one-dimensional simulation using the numerical codes developed by Wilson and Mayle [5]. Since we use the Livermore results as input for our evaluation of the response of an underwater Cherenkov detector, we recall the main features of the expected neutrino signal.

During the simulated time interval of 18 s after bounce, the total energy emitted is 2.9×10^{53} erg . Fig. 1 represents the neutrino luminosities and average energies for the first 1.5 s, during which the main signatures of collapse and delayed explosion can be individuated.

The early spike in ν_e light curve is due to the prompt neutrino burst that is generated when the shock passes through the neutrino trapping zone in the core, inferring the iron dissociation and the subsequent neutronization of the involved layer.

The following accretion phase holds while the material falls in and feeds the neutrino emission, and in the Livermore results lasts until about 0.5 s. During the accretion phase the luminosity of all neutrino species drops abruptly due to the increasing opacity of the infalling matter that accretes the protoneutron star. In the same time the average energy increases because the mass accretion rate decays gradually. These two features are considered the characteristic signatures of a delayed explosion mechanism.

The third phase, beyond 0.5 s, is the cooling of the new born neutron star by neutrino emission, characterized by luminosity values well below the previous ones.

Comparing the time evolution of L_{ν_e}, $L_{\overline{\nu}_e}$ and L_{ν_x} (where ν_x represents ν_μ, $\overline{\nu}_\mu$, ν_τ and $\overline{\nu}_\tau$) we find out that after the first 0.1 s the energy is roughly equipartitioned among all neutrino flavours. The comparison among the average energies shows the usual hierarchy $\langle E_{\nu_e} \rangle < \langle E_{\overline{\nu}_e} \rangle < \langle E_{\nu_x} \rangle$ that reflects the corresponding order in the emission neutrinospheres.

Concerning the spectra (see Fig. 2), one can easily see the difference between the numerical results and the thermal Fermi-Dirac (F-D) fit, defined as:

$$n_\nu(E) = AT^3E^2\left[1+\exp\frac{E}{T}\right]^{-1}, \tag{1}$$

where A is a constant, T is the temperature of the spectrum and E is the neutrino energy, the last two quantities being expressed in MeV.

We want to underline that the F-D curves lead to a general overestimation of both low and high energy events; for this reason we adopted the numerical spectra rather that thermal F-D ones, often used for analogous simulations.

3 Interaction of low-energy neutrinos in water

When the low-energy neutrinos coming from a SN event pass through the water volume of a detector, they can interact with the constituents of water. The interaction processes of interest in water Cherenkov detectors are:

$\overline{\nu}_e + p \rightarrow e^+ + n$	$(\varepsilon_\nu^{th} = 1.8$ MeV$)$	(CC)
$\nu_e(\overline{\nu}_e) + e^- \rightarrow \nu_e(\overline{\nu}_e) + e^-$		(CC+NC)
$\nu_x + e^- \rightarrow \nu_x + e^-$		(NC)
$\nu_e + {}^{16}O \rightarrow e^- + {}^{16}F$	$(\varepsilon_\nu^{th} = 15.4$ MeV$)$	(CC)
$\overline{\nu}_e + {}^{16}O \rightarrow e^+ + {}^{16}N$	$(\varepsilon_\nu^{th} = 11.4$ MeV$)$	(CC)

where ε_ν^{th} is the threshold energy of neutrinos, NC indicates a process that goes through Neutral Current interaction, and CC a Charged Current one. Comparing the total cross-sections of the above reactions in the energy range of interest and taking into account the different abundances of such targets in water, we see that inverse β decay is the dominant process [11].

Several works concerning the evaluation of the response of a water Cherenkov detector consider that the positrons emitted in inverse β decay processes are distributed isotropically. In principle, an underwater detector as the one under examination, since composed by couples of upward-downward OMs, could discern an asymmetry in the emitted Cherenkov light.

In order to evaluate whether is possible to reconstruct the SN direction or not, we adopted the angular distribution of the inverse β decay calculated by Beacom and Vogel [12,13]. If ϑ is the angle between the directions of the incident $\overline{\nu}_e$ and of the outgoing e^+ in the laboratory system, they found at first order in $1/M$ (where M is the proton mass in MeV$/c^2$ and $c = 1$ units):

$$\langle \cos\vartheta \rangle^{(1)} \simeq -0.034 v_e^{(0)} + 2.4 \frac{E_\nu}{M}, \tag{2}$$

where $v_e^{(0)}$ is the zero-th order e^+ velocity (in $c = 1$ units) and E_ν is the $\overline{\nu}_e$ energy in MeV.

The resulting angular distribution is slightly backward for $E_\nu < 15$ MeV, while above this limit the distribution becomes forward peaked. However, we remark that in the whole range of our interest ($0 \div 30$ MeV) this asymmetry is weak, since $|\langle \cos\vartheta \rangle| < 0.05$.

4 Adopting a geometry: the NEMO project

In this section we briefly describe the detector geometry adopted in the present work, according to one of the candidate geometries for the NEMO (NEutrino Mediterranean Observatory) project. A complete description of the NEMO project and of the various detector geometries proposed can be found in Refs. [14] and [15].

In the present work, we choose a geometry composed by 64 "towers", placed in an array having a step of 200 m in seawater. A single tower is composed by 16 floors, 40 m distant, each one containing two couples of up/down looking Optical Modules (OM), held at the end of a beam 20 m long. Each beam forms a right angle with the contiguous one. The effective height of the tower is so 600 m, to which a distance of 150 m between the first floor and the sea bottom has to be added, giving a total height of 750 m.

The described detector would have a physical volume of $1400 \times 1400 \times 600$ m $= 1.176 \cdot 10^9$ m^3, instrumented with 4096 OMs.

In the configuration adopted, each OM contains a 8" photomultiplier tube (PMT) enclosed in a glass sphere and optically coupled with it by means of an optical gel.

5 Monte Carlo simulation of the detector response

To evaluate the response of the previously described neutrino telescope, we developed a Monte Carlo code simulating the whole detection process.

We adopted the $\overline{\nu}_e$ flux calculated by the Livermore group [10] to evaluate the number of e^+ that in a second are emitted in the detector volume ($1.2 \cdot 10^9$ m^3 of water) as a function of time:

$$\frac{dN_{e^+}(t)}{dt} = \frac{L_{\overline{\nu}_e}(t)}{\langle E_{\overline{\nu}_e}(t) \rangle} \cdot \frac{l^2}{4\pi d^2} \cdot (1 - e^{-\frac{h}{\lambda}}). \tag{3}$$

Here $L_{\overline{\nu}_e}(t)$ and $\langle E_{\overline{\nu}_e}(t) \rangle$ are the $\overline{\nu}_e$ luminosity and average energy (see Fig. 1), d is the SN distance, l and h are the detector side (1400 m) and height (600 m), and $\lambda = (n\sigma^{-1})$, where n is the number of targets (p) in the unitary water volume ($n = 6.692 \cdot 10^{28}$ [m^{-3}])

and σ is the total cross section from [11]. All the above mentioned physical quantities are intended in the proper SI units.

In Fig. 3 we show the comparison between $dN_{e^+}(t)/dt$ for a SN located at the Galactic center ($d = 10$ kpc) and at the LMC distance ($d = 50$ kpc). The integrals of such curves, i.e. the number of e^+ generated in $t = (0 \div 10)$ s are $3.1 \cdot 10^8$ and $1.2 \cdot 10^7$ respectively.

We also notice that, due to the increasing $\langle E_{\overline{\nu}_e} \rangle$ with time (see Fig. 1), the $dN_{e^+}(t)/dt$ curve does not show a parallel behaviour with respect to the $L_{\overline{\nu}_e}(t)$ one, superimposed in Fig. 3. When $E_{\overline{\nu}_e}$ becomes higher, σ for inverse β decay increases too [11,12], and this fact leads to an enhancement of the e^+ production in the detector volume in correspondence of the accretion and cooling phases of the stellar collapse. However, the smooth rise of σ in the neutrino energy range explored leaves unaltered the main features of the signal expected.

We assumed that the angular distribution of the emitted e^+ changes according to 2. Each e^+ can interact in water via Coulomb scattering, bremsstrahlung, Cherenkov effect, and finally it annihilates with an electron. The path between creation and annihilation vertices is few tens cm long. The simulation follows all resulting γ and $e^\pm$ down to $E_\gamma = 10$ keV and $E_{e^\pm} = 10$ keV.

The emitted Cherenkov photons must be propagated inside the detector volume, in which three main processes can occur: i) absorption in the volume detector; ii) escaping from the same volume; iii) detection by the OMs.

We accounted for absorption in seawater adopting the absorption length values measured by the NEMO collaboration in the "KM4" site in front of Capo Passero (Sicily) [18], according to which a maximum value of the absorption length of 65 m is assumed. We neglected the light diffusion due to Rayleigh and Mie scattering, also present in seawater, because the very small scattering angle typical of such processes do not influence significantly the overall angular distribution of the Cherenkov light, already almost isotropical.

We have an hit on a PMT when a Cherenkov photon arriving on it leads to a photoelectron count in the electronic output chain. By using the absorption properties and OM specifications stated in Section 4, we obtained the results presented in Figs. 4 and 5 for a SN located at $d_{SN} = 10$ kpc that explodes at the detector zenith.

We calculated the frequency of hits summed over the 2048 upward-looking PMTs (F_{up}) and over the 2048 downward-looking PMTs (F_{down}) in order to evaluate the possibility to get information about the SN direction from the up/down asymmetry defined as:

$$A = \frac{F_{up} - F_{down}}{F_{up} + F_{down}}. \quad (4)$$

Unfortunately, as can be deduced from the almost perfect superimposition between F_{up} and F_{down} in Figs. 4 and 5, the asymmetry parameter A is very small, even in the most favourable case for us, i.e. a SN located at the detector zenith.

For this reason we can conclude that is not possible to retrieve any useful information about the SN direction through the analysis of the angular distribution of the Cherenkov light. In other words, the results shown in Figs. 4 and 5 are independent of the SN position in the sky.

6 Facing with background: a statistical analysis

When we consider a real experiment, we must face with several sources of noise among which our signal has to be discerned.

^{40}K is a β^- emitting radionuclide melted in seawater, and, in small percentage, also in the glass spheres of the OMs.

The e^- emitted by ^{40}K in seawater produce Cherenkov light as well as e^+ from inverse β decay processes induced by SN events; consequently those processes have the same statistical behavior, that we consider as Poissonian. The ^{40}K decays in glass produce scintillation [16], a non-Poissonian process that is described in detail in Ref. [17].

For the seawater ^{40}K we suppose an average counting rate of 30 kHz, which is the value measured for 8" PMTs by the NEMO collaboration in the "KM4" site in front of Capo Passero (Sicily) [18], while from the ^{40}K content in glass spheres we expect about 1 kHz rate [16]: so this second process yelds in a deep undersea detector a noise rate more than an order of magnitude lower than the first one, and consequently can be neglected in our calculations.

Another important source of noise in an underwater experiment is bioluminescence, i.e. the light emitted by biological sources, that is under study and evaluation by various collaborations [18]. Bioluminescence seems to have a twofold nature: on the first hand we have light emitting bacteria and microorganisms, that populate large volumes of water and move slowly in a collective way as clouds carried by the sea currents; on the other hand we have abyssal fishes and macroscopic organisms that can pass through the detector towers. These two kinds of bioluminescent sources lead to different kind of noise in the detector: the first one can lead to an increase in the average counting rate on very large sections of the array on timescale of the order of hours, and can be accounted for using a "Moving Average" method as the one described in [16]. The second signal instead leads

to a large increase in the counting rate on small groups of adjacent OMs in timescale of the order of seconds, and can be rejected since it is very different from the average counting rate of the whole detector.

The measurements carried out by the NEMO collaboration [18] show that the background counting rate present quite rare fluctuations due to bioluminescence; in particular, the measurements performed in front of Capo Passero show that the presence of luminescent bacteria below 2500 m is negligible.

It must pointed out explicitly that such considerations about triggering could apply only for SN detection, that is the purpose of our study, while for the reconstruction of high energy neutrino events different cuts in general can be necessary.

When a SN event occurs, the counting rate due to SN $\overline{\nu}_e$ adds upon the ^{40}K background rate; if the SN distance is not too large, the early brightest phase of SN signal should emerge from Poisson fluctuations of noise.

In the following we indicate with $F^d_{SN}(t)$ the frequency [Hz] of hits on all 4096 PMTs, for a SN exploding at distance d [kpc]. As can be seen in Fig. 4 at $t_{MAX} \simeq 0.25$ s we have:

$$F^{10}_{SN}(t_{MAX}) = F_{up} + F_{down} \simeq 1.6 \cdot 10^6 \text{Hz}, \tag{5}$$

that is the maximum frequency of hits for the adopted SN model, exploding at $d = 10$ kpc on the detector zenith.

$F_{^{40}K}$ is the total frequency of noise hits due to ^{40}K, i.e.:

$$F_{^{40}K} = 4096 \cdot 3 \cdot 10^4 \text{Hz} = 1.23 \cdot 10^8 \text{Hz}. \tag{6}$$

In order to maximize the signal to noise ratio, and consequently maximize the detection horizon, is necessary to integrate the counting rate over a suitably chosen time interval Δt [s].

Let be $n^d_{SN}(t) = F^d_{SN}(t) \cdot \Delta t$ and $n_{^{40}K} = F_{^{40}K} \cdot \Delta t$; the statistical significativity can be defined as:

$$S(t) = \frac{n^d_{SN}(t) + n_{^{40}K} - n_{^{40}K}}{\sigma(n^d_{SN}(t) + n_{^{40}K})} = \frac{n^d_{SN}(t)}{\sigma(n^d_{SN}(t) + n_{^{40}K})}. \tag{7}$$

To ensure detection, we can require that the signal at its maximum exceeds the ^{40}K background at least 3 times its fluctuation, i.e. we can require that:

$$S(t_{MAX}) = 3 = \frac{F^{oriz}_{SN}(t_{MAX}) \cdot \Delta t}{\sqrt{(F_{^{40}K} + F^{oriz}_{SN}(t_{MAX})) \cdot \Delta t}}, \tag{8}$$

where $F_{^{40}K}$ is from Eq. 6 and $F_{SN}^{oriz}(t_{MAX})$ is the corresponding maximum frequency of hits yelded by a SN at the detection horizon. Consequently we can find a relationship between $F_{SN}^{oriz}(t_{MAX})$ and Δt:

$$\Delta t = 1.11 \cdot 10^{9} \left[F_{SN}^{oriz}(t_{MAX})\right]^{-2} + 9 \left[F_{SN}^{oriz}(t_{MAX})\right]^{-1}. \tag{9}$$

Recalling that the ν emission from SN is isotropic, we can rescale our result of $F_{SN}^{10}(t_{MAX})$ obtained in Eq. 5 for $d = 10$ kpc to the detection horizon R_{oriz} [kpc]:

$$F_{SN}^{oriz}(t_{MAX}) = 1.6 \cdot 10^{6} \cdot \frac{10^{2}}{R_{oriz}^{2}}. \tag{10}$$

Substituting in 9 we obtain:

$$\Delta t = 4.34 \cdot 10^{-8} R_{oriz}^{4} + 5.62 \cdot 10^{-8} R_{oriz}^{2}. \tag{11}$$

A more conservative relationship can be obtained imposing in Eq. 8 $S(t_{MAX}) = 5$:

$$\Delta t = 1.20 \cdot 10^{-7} R_{oriz}^{4} + 1.56 \cdot 10^{-7} R_{oriz}^{2}. \tag{12}$$

The relations 11 and 12 are plotted in Fig. 6 in the $(10 \div 25)$ kpc range. Since we assumed that during the integration time interval Δt the signal F_{SN} remains constant, we cannot adopt an arbitrarily long value for Δt itself. Anyway, Fig. 6 shows that a Δt of the order of 10^{-2} s is enough to ensure the detection of a SN in the entire Galaxy.

7 Summary and conclusions

We performed a complete Monte Carlo simulation of the response of a realistic model of a deep-undersea Cherenkov detector to low energy neutrinos from a $20\ M_{\odot}$ SN progenitor.

Having individuated in the inverse β decay the dominant process for such a detection, we adopted a detailed treatment for that reaction and for the tracking of the emitted e^{+}, secondaries, and Cherenkov photons.

The expected increase in the total counting rate of the entire array has been compared with the different sources of noise. We found that ^{40}K is the main source of noise, being bioluminescence more easily accountable by properly chosen methodologies.

By applying to the MC data a statistical treatment based on the integration of the frequency of hits over a properly chosen time interval, we found that a time interval of the order of 10^{-2} s is large enough to ensure the detection of a Galactic SN.

Moreover, it is almost impossible to retrieve any useful information about the SN direction observing the angular distribution of the Cherenkov light in the array by using the up/down configuration of the OMs of the considered detector.

Working on the total counting rate of all OMs, the entire SN detection principle described holds on the technical capability of the experiment to sum over the OMs and integrate the background rate, analyzing online the results in the framework of an international SN alert network.

This ambitious aim probably could be achieved by adopting the most recent electronic configurations today available, and the results of studies like ours can suggest the requirements necessary to make the future ultra-high energy neutrino telescopes [14] [19] [20] sensitive to SN events.

References

[1] G. E. Brown, H. A. Bethe, G. Baym, Nucl. Phys. A **375** (1982) 481

[2] S. E. Woosley, T. A. Weaver, Ann. Rev. Astron. Astrophys. **24** (1986) 205

[3] H. A. Bethe, J. R. Wilson, ApJ **295** (1985) 14

[4] H. T. Janka, Astron. Astrophys. **368** (2001) 527

[5] R. Mayle, J. R. Wilson, D. N. Schramm, ApJ **318** (1987) 288

[6] G. G. Raffelt, Nucl. Phys B (Proc. Suppl.) **110** (2002) 254

[7] M. Rampp, H. T. Janka, ApJ **539** (2000) L33

[8] A. Mezzacappa, astro-ph/0010580

[9] M. Liebendorfer, A. Mezzacappa, F. K. Thielemann, O. E. B. Messer, W. R. Hix, S. W. Bruenn, Ph. Rev. **D63** 103004 (2001)

[10] T. Totani, K. Sato, H. E. Dalhed, J. R. Wilson, ApJ **496** (1998) 216

[11] W. C. Haxton, Ph. Rev. **D36** (1987) 2283

[12] P. Vogel, J. F. Beacom, Ph. Rev. **D60** (1999) 053003

[13] J. F. Beacom, P. Vogel, Ph. Rev. **D60** (1999) 033007

[14] NEMO Collaboration, The NEMO Project, http://nemoweb.lns.infn.it/project.htm

[15] C. De Marzo for the NEMO.RD Collaboration, Nucl. Phys. B (Proc. Suppl.) **87** (2000) 433

[16] AMANDA Collaboration, Astropart. Phys. **16** (2002) 345

[17] B. E. A. Saleh, J. T. Tavolacci, M. C. Teich, IEEE J. Quant. Elec. **QE-17** (1981) N. 12, 2341

[18] NEMO Collaboration, Study and characterization of a deep sea site for a km3 underwater neutrino telescope, http://nemoweb.lns.infn.it/sitereport

[19] S. E. Tzamarias, NIM A **502** (2003) 150

[20] G. D. Hallewell, NIM A **502** (2003) 138

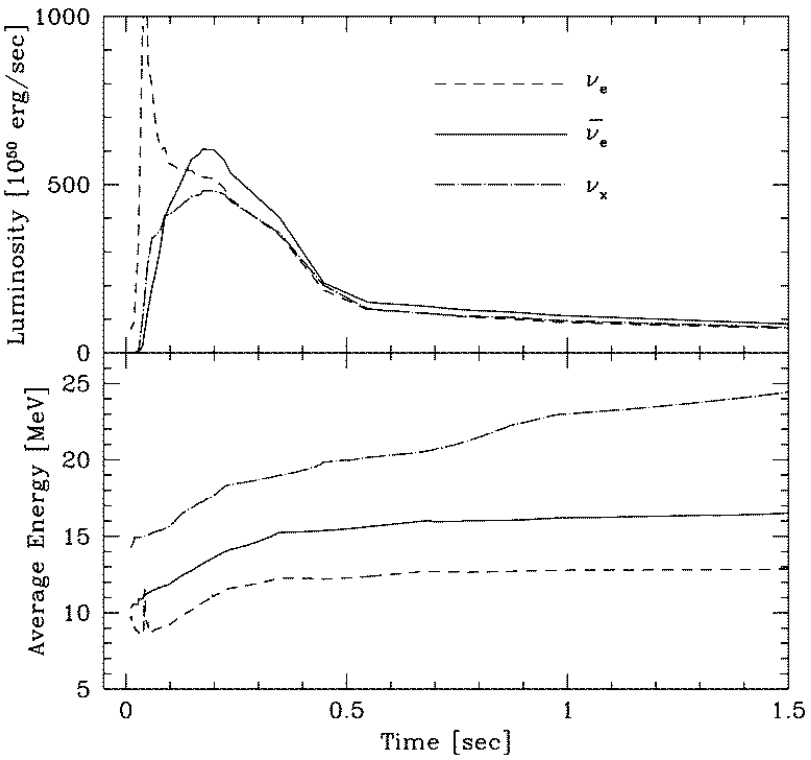

Figure 1: Time evolution of neutrino luminosity and average energy from [10].

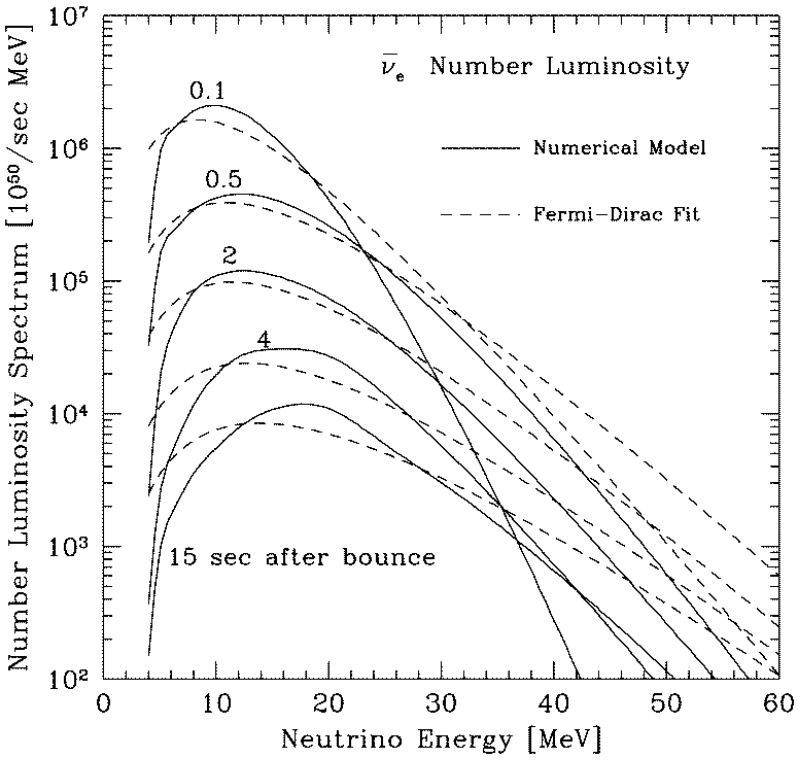

Figure 2: Energy spectra of $\overline{\nu}_e$ at five times indicated. The dashed lines are F-D fits. [10].

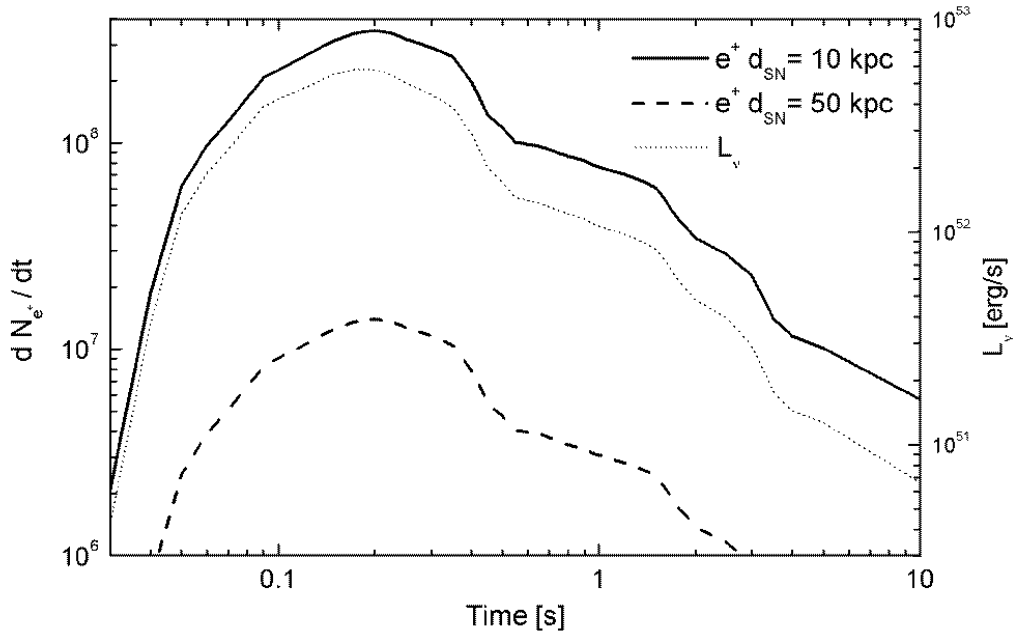

Figure 3: e^+ frequency in the detector for a source located at 10 kpc (solid line) or at 50 kpc (dashed line). $L_{\overline{\nu}_e}$ from [10] is superimposed as dotted line for comparison (see text).

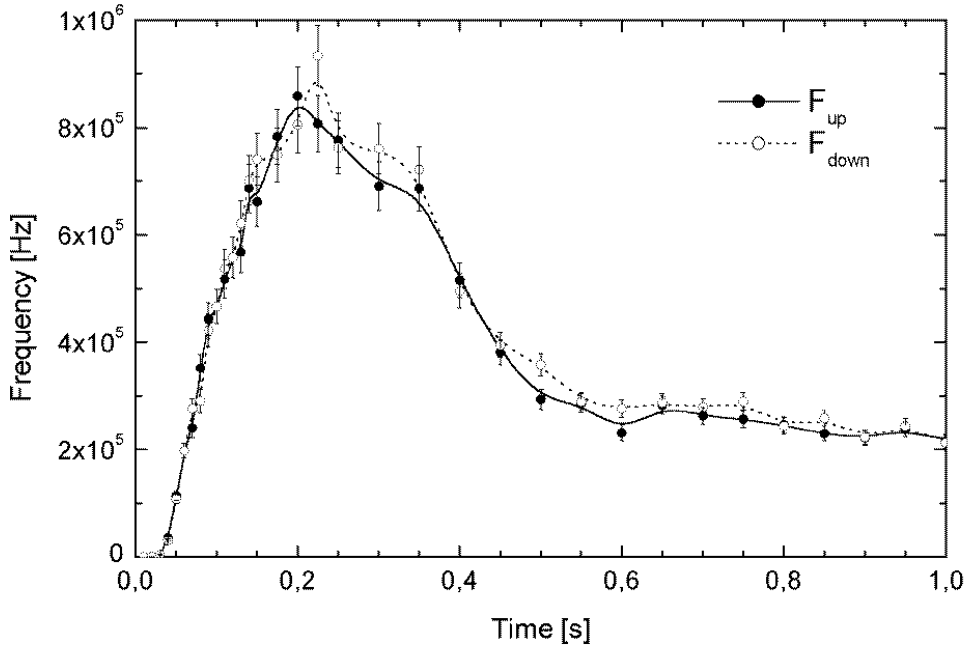

Figure 4: Frequency of hits on the 2048 PMTs up (F_{up}) and down (F_{down}) for a SN located at 10 kpc exploding at the detector zenith. Solid and dashed lines are to be intended as guides for eyes.

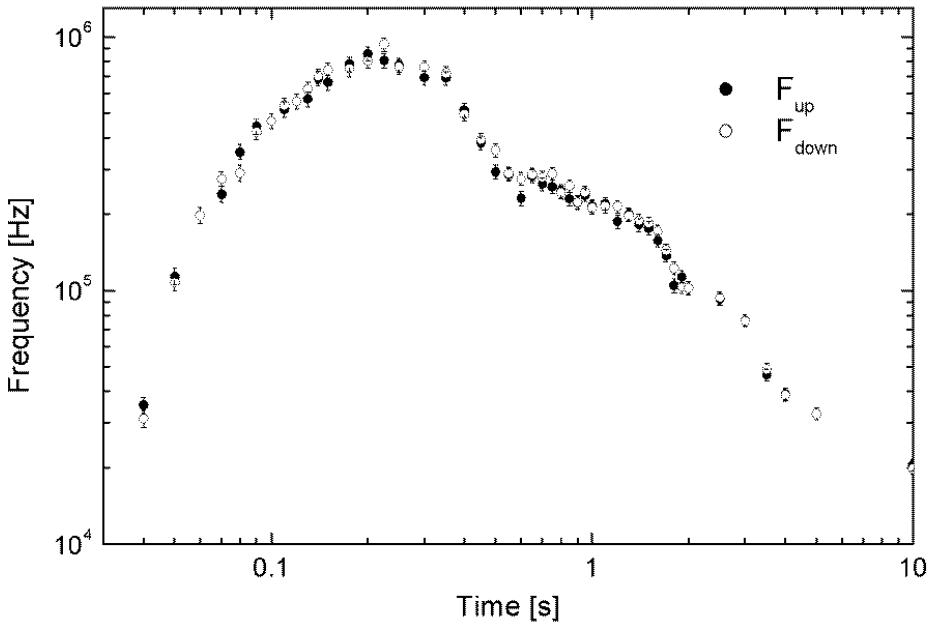

Figure 5: Same as 4 for the whole simulation time interval.

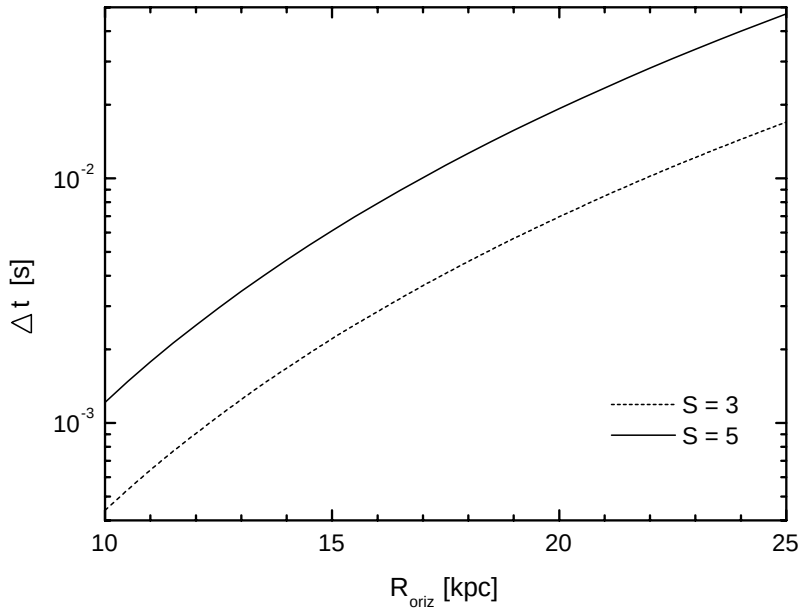

Figure 6: Detection horizon R_{oriz} [kpc] vs. integration time interval Δt [s] according to Eq. 11 and 12.